J Fluoresc (2008) 18:1083–1091
DOI 10.1007/s10895-008-0353-y

ORIGINAL PAPER

Nile Red Synchronous Scan Fluorescence Spectroscopy to Follow Matrix Modification in Sol–Gel Derived Media and its Effect on the Peroxidase Activity of cytochrome *c*

Ana Rei · M. Isabel C. Ferreira · Graham Hungerford

Received: 5 November 2007 / Accepted: 19 February 2008 / Published online: 26 March 2008

Abstract The highly solvatochromic dye Nile red is used in conjunction with synchronous scan fluorescence spectroscopy to elucidate changes in the internal environment of cytochrome *c*, upon incorporation into differently modified sol–gel derived media. Nile red was first studied in a variety of solvents in order to quantify changes in polarity. Matrix modifications involved the addition of several silanes, intended to interact with any unreacted hydroxyl entities left from the matrix forming reaction, while polymers were used to help reduce shrinkage and modify the internal pore environment. Slight unfolding of the protein was observed on incorporation into the sol–gel derived media. During the aging process further changes were monitored by using difference synchronous scan fluorescence spectra and complementary measurements of catalytic activity, expressed as the initial velocity. Combining Nile red synchronous scan fluorescence with cytochrome *c* activity data lead to a method to elucidate effects linked to protein conformation and those related to the sol–gel derived host.

Keywords Nile red · Silanes · Polymers · Synchronous scan fluorescence spectra · Sol–gel monolith · Catalytic activity

Electronic supplementary material The online version of this article (doi:10.1007/s10895-008-0353-y) contains supplementary material, which is available to authorized users.

A. Rei · M. I. C. Ferreira · G. Hungerford (✉)
Departamento de Física, Universidade do Minho,
4710-057 Braga, Portugal
e-mail: graham@fisica.uminho.pt

G. Hungerford
Physics Department, King's College London,
Strand, London WC2R 2LS, UK

Introduction

The use of sol–gel derived media [1, 2] for the incorporation of biomolecules has recently proved to be an active field of investigation [3–9]. Although these media can provide good hosts for enzymes because of their low processing temperatures, robustness, and high degree of porosity [1], significant improvements are needed to make these materials common biosensor hosts. In fact, the modification of these glass-like materials may produce more amenable microenvironments in which to host biomolecules. Important factors to address are; matrix shrinkage, presence of alcohol as a by-product from the matrix forming reaction and the internal pore environment, in terms of retained solvents and unreacted groups [10]. Strategies to overcome adverse factors include the use of biocompatible polymers, such as poly (ethylene glycol) [11], chitosan [12], glycerol derived systems [13, 14] and polysaccharides [15]. Functionalising sol–gel derived silica media by the addition of different silanes has also shown to be advantageous [16].

A suitable biomolecule to be used in order to assess the effect of matrix modification is the haem containing cytochrome *c* [17, 18], a protein involved in the electron transfer process in cellular respiration. It has previously been used to probe the internal environment of sol–gel derived media [19] and its conformation monitored during the host aging [20]. Since the sol–gel method provides transparent matrices of good optical quality, spectroscopic techniques to monitor both the matrix and the entrapped biomolecule can be successfully used. In fact, the authors have previously made use of the solvatochromic properties of dye Nile red [21–23] to monitor the incorporation of horseradish peroxidase into sol–gel derived media [24, 25]. This study has shown that the photophysics of Nile red is

well suited to elucidate changes in protein conformation. Moreover, this dye has previously been used in conjunction with synchronous scan fluorescence spectroscopy (SFS) [26, 27] to ascertain the probe distribution between lipoproteins and albumin in blood [28]. Therefore, Nile red emission examined by SFS appears promising considering the solvatochromic nature of the dye and the ability of SFS to resolve components from mixtures of distinct fluorescent species.

In the present work incorporation of cytochrome *c*, at a relatively low loading, into several modified sol–gel derived hosts was monitored *via* Nile red emission in conjunction with synchronous scan fluorescence spectroscopy. A study of the SFS of Nile red in solvents of differing dielectric constants was first made, to produce a reference scale. This enabled the microenvironments probed by the entrapped dye to be discriminated throughout the aging process of the sol–gel derived hosts. The materials produced were based on a previous reaction procedure using tetraethylorthosilicate to form a sol [24], modified by the incorporation of either poly(ethylene glycol) or Gelrite® or aminopropyl triethoxysilane (APTES) or trimethoxypropylsilane (TMPS) or glycidyloxypropyl triethoxysilane (GPTES) prior to gelation. The effect of these modifiers upon the activity of cytochrome *c* was monitored through the aging process.

Experimental

Sample preparation

Sols were manufactured as we have previously reported [24, 29], based on the method given by Flora and Brennan [30]. Cytochrome *c* (horse heart, Aldrich) was either used as received or labelled with Nile red by taking 0.3 mg of protein in 2 ml of phosphate buffer solution (pH 7) and incubating with 2 μl of 10^{-3} M solution in dimethylsulfoxide for 1 h. The hybrid hosts were then manufactured using 10 mm pathlength polystyrene cuvettes (*ca*. 4.5 ml volume) by taking 2 ml of sol and adding silane (150 μl for TMPS and GTPES, 20 μl for APTES), polymer (1 mg of PEG 20 kDa, 0.1 ml PEG 300) or Gelrite® (0.6 mg) and 2 ml of the protein solution. After combining the mixtures, the cuvette was sealed with parafilm and the solution mixed by inverting. The solution gelled within minutes and was stored between measurements at 4 °C with the top of the cuvette covered. Under these conditions an average shrinkage of *ca*. 40% occurred during the experiment period and the matrices exhibited a good optical quality. Nile red was purchased from Aldrich. The additives, ((3-Aminopropyl) triethoxysilane, Trimethoxy(propyl)silane and (3-Glycidyloxypropyl) triethoxysilane) were all acquired from Sigma, Aldrich or Fluka, as was Poly(ethylene glycol) (PEG, molecular weights 300 and 20,000) and Gelrite®. All were used as received. The structure of Nile red, along with those of the additives, is shown in Scheme I.

Catalytic activity

A measurement of cytochrome *c* activity was obtained from the oxidation of ABTS (2,2-Azino-bis(3-ethylbenzothiazoline-6-sulfonic acid) diammonium salt, from Sigma) by hydrogen peroxide (H_2O_2, 37% Aldrich). Activity measurements in aqueous solution served as reference to the measurements involving the sol–gel matrices and were performed using differing quantities of enzyme with a fixed substrate concentration. For the studies on the sol–gel derived systems, 100 mg of matrix (a slice cut from the monolith) was taken and added to a cuvette containing 2 ml of 2.5×10^{-5} M ABTS and 8 μl H_2O_2 in buffer solution. The absorption spectrum was recorded in the range 250–500 nm, both before the addition of the matrix and after the kinetic study was complete. The kinetic studies commenced either on the addition of the cytochrome *c* or protein containing matrix and followed the formation of the ABTS radical by monitoring absorption changes at 414 nm [10, 31].

Measurements

Spectra were recorded using a Shimadzu UV-3101PC (absorption) and a SPEX Fluorolog spectrophotometer (fluorescence). Synchronous scan fluorescence spectra were measured by scanning both the excitation and emission

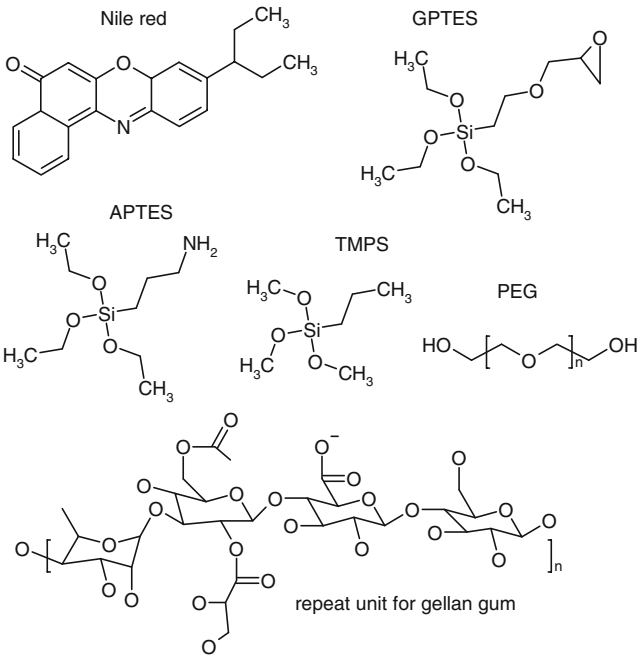

Scheme I Chemical structures of Nile red and additives

simultaneously with a constant wavelength difference between them. This has the effect of producing a spectrum that is a combination of both the absorption and fluorescence emission [27]. The resulting spectra are shown giving the wavelength of the excitation. Initially wavelength offsets of 10, 20 and 50 nm were employed. A difference of 20 nm between the excitation and emission monochromators was then chosen for the study. This technique has proved adept in analytical applications [26]. Difference spectra were calculated by normalising the spectra and subtracting from the reference spectrum. All measurements were performed at ambient temperature and taken over a 40 day period to check for longer term changes during sol–gel host aging.

Results and discussion

Nile red SFS in solution

In order to make use of Nile red's solvent sensing e.g. solvatochromic properties, a synchronous scan study was first performed in a range of solvents (see supporting information for solvent details). Initially three different wavelength offsets were employed, as shown in Fig. 1 for three solvents. In a solvent of low polarity, such as hexane, the greater offset spectrum is more structured, because of the vibrational features present in both the normal absorption and emission spectra [32]. This structure reduces with a reduction of the offset between the excitation and emission wavelengths and is lost when an offset of 10 nm is used. In higher polarity media, the spectra at the three different offsets all exhibit a Gaussian band shape, not surprising as the normal absorption and emission spectra do not exhibit vibrational structure. It should be noted that the

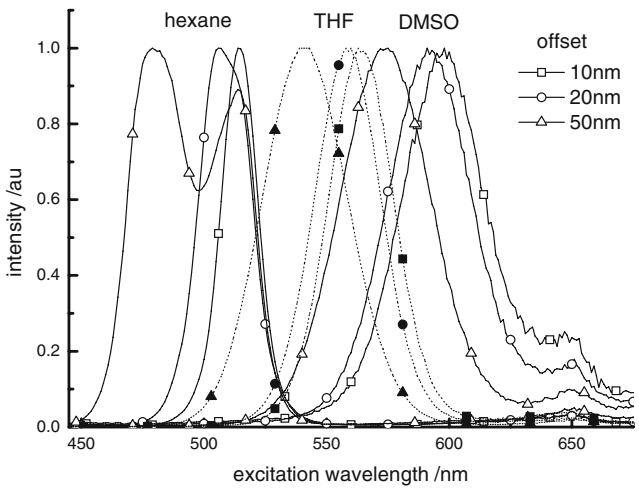

Fig. 1 Effect of wavelength offset (10 nm *squares*, 20 nm *circles*, 50 nm *triangles*) on synchronous scan spectrum of Nile red in a solvent of low (*hexane*), moderate (*THF—dotted lines*) and high (*DMSO*) dielectric constant. The spectra are shown normalised

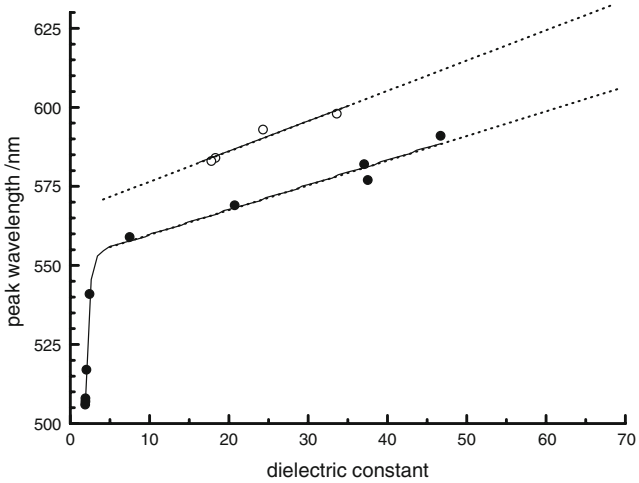

Fig. 2 Peak wavelength obtained from the synchronous scan spectra of Nile red in various solvents of differing dielectric constants. The data for alcohols are shown by *open symbols*. *Lines* are for guidance (*solid lines* fitted to data, *dotted lines* show trends only)

feature (small band) situated at 650 nm is present throughout and hence may relate to an artefact and thus will be ignored for the purpose of this paper. A compromise offset of 20 nm was chosen for a larger study as this could also indicate if the spectra possessed any vibrational structure, while producing an easily identifiable peak. The outcome is shown in Fig. 2 and the observed trend is in accordance with studies using the Nile red fluorescence emission [22, 23, 29]. Therefore, in adopting SFS of Nile red with the 20 nm offset, it is possible to obtain an "easy to use local polarity sensor".

Figure 2 clearly shows a relationship between the peak position of the synchronous scan spectrum and the dielectric constant of the solvent used. As expected, the behaviour in alcohols (shown by open symbols in Fig. 2) is different [33] and a red shift is observed for this class of solvents in comparison to the others of similar dielectric constant. It is notable that using this technique, small changes in relatively low values of dielectric constant produce a relatively large change in spectral position. However, it should be noted that a constant wavelength offset is used, as the apparatus does not allow the use of a constant energy offset set up. At higher values of dielectric constant (greater than 10) smaller peak shifts are observed. These data provide an expedient means by which to "quantify" changes in dielectric constant and to "estimate" the contribution of hydrogen bonding in the measured spectral shifts, over a range of polarities pertinent to the present system.

Protein incorporation within sol–gel derived media

Three sets of samples were produced, one containing cytochrome *c* which had been incubated with Nile red for use in the fluorescence study (referred to as NR-cyt-matrix

acronym) and another with unlabelled protein (Cyt-matrix acronym) for use in activity studies. A further set of samples was produced containing Nile red, but no protein (NR-matrix acronym). All samples were kept under the same ambient conditions throughout the experiment.

In order to ascertain the behaviour of cytochrome *c* when incorporated into each sample, the fluorescence of Nile red labelled protein was also examined and compared with its behaviour in buffer solution. Figure 3 shows the Nile red SFS measurements for both sets of dye containing samples, just after the gelation of the host media. The spectrum obtained for Nile red in cytochrome *c* in buffer solution is also given for comparison (Fig. 3b).The spectra are shown normalised at each maximum, to emphasise environmental changes, expressed by band position. Such methodology was adopted to overcome slight increases in the concentration of the entrapped species caused by matrix shrinkage. Figure 3a shows that, in absence of the protein, NR probes a very polar medium, with an "equivalent" dielectric constant in the order of 60, according to Fig. 2. This behaviour indicates that, most probably, Nile red probes an environment influenced by the high dielectric constant of the aqueous buffer solution as expected at this early stage of the gelation process, when the matrix network is still embedded in the initial solvent medium. On the other hand, Fig. 3b shows that, whenever cytochrome *c* is present, Nile red probes a wider range of local polarities; in fact the Nile red emission is now characterised by the presence of three bands centred at 500, 550 and 615 nm. The occurrence of the three bands indicates that, in presence of the protein, the hydrophobic Nile red [34], is located within the protein network, either in its periphery and more polar region, as shown by the 615 nm band, or in less polar regions of the protein, as indicated by the 550 and 500 nm bands. The fact that the probe is not covalently bound to the protein, favours its mobility and thus its capacity to report on a range of distinct local environments.

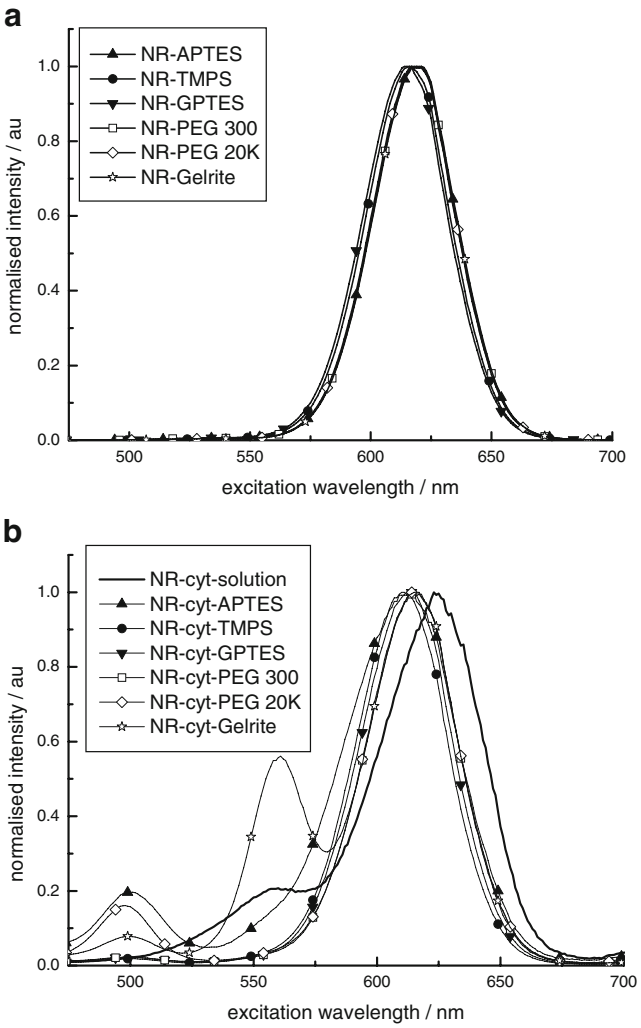

Fig. 3 Normalised Nile red SFS data obtained with an offset of 20 nm, **a** Nile red in the different host media, **b** Nile red in cytochrome *c* in solution and just after incorporation of the protein into the sol–gel derived media

Overall, the relative intensities of Nile red in the presence of protein were significantly lower than in the matrices produced with the dye in the absence of cytochrome *c* (see supporting information). These results indicate that a significant part of the dye emission is extinguished by the presence of the protein. It is important to note that the authors have previously found evidence for fluorescence resonance energy transfer between Nile red and the haem group in horseradish peroxidase [23]. Considering the smaller size of cytochrome *c*, approximately spherical in water with dimensions $15\times15\times17$ Å^3 [35], it is highly likely that fluorescence energy transfer from Nile red to the Q bands of the haem group of the protein is responsible for the lower intensities observed for Nile red in presence of this protein. The relative intensity of the Nile red bands, shown in Fig. 3b, corroborates further the RET mechanism, since the 500–550 nm bands of Nile red overlap with the *Q* bands of cytochrome *c* [36].

The results, shown in Fig. 3, point out to the fact that negligible leaching of Nile red and/or unfolding of the protein occurred under these experimental conditions. In fact denaturing of the cytochrome *c* with with 6.5 M urea (see supporting information) showed an increase in the dye emission intensity of about ten times, along with a slight red shift and narrowing of the emission peak. This is consistent with the protein unfolding, causing a decrease in Nile red-haem energy transfer and the probe sensing a slight increase in polarity as the protein structure opens. These results are contrary to those given in Fig. 3b. Finally, it should be noted that the band centred at 560 nm becomes more prominent in the Gelrite containing host, thus hinting that energy transfer from the 560 emission band of Nile red

is less efficient in this matrix. However the main features described in this section apply to all hosts.

Protein conformation and catalytic activity during the aging process

Nile red SFS

Nile red SFS for each of the hosts was measured at regular intervals over an aging period of more than forty days (see supporting information). Figure 4 illustrates the shifts in the Nile red maximum wavelength for each matrix as the aging progresses. Figure 4a shows that in absence of cytochrome *c* Nile red emission displays one maximum, characteristic of a polar medium. As the aging progresses a red shift is observed in all hosts except for the TMPS matrix. The behaviour of the cytochrome *c* containing samples (Fig. 4b) shows that the main environments probed by Nile red remain relatively constant throughout the time period of this study. Most probably, incubation of Nile red into the protein structure protects the hydrophobic dye from probing the chemical changes that occur during the aging process [1]. In fact the results presented in the previous section support the idea that leaching of the dye is negligible.

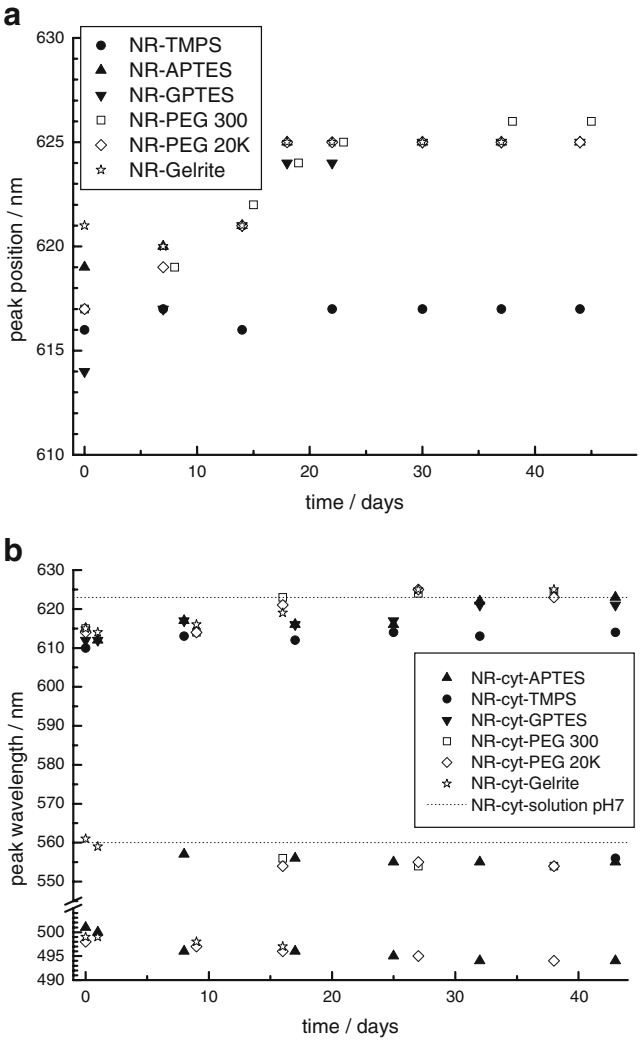

Fig. 4 Synchronous scan spectra (20 nm offset) for Nile red **a** in hosts without protein and **b** in cytochrome *c* incorporated within differently modified matrices. The *dotted lines* in (**b**) indicate the position of the peak and shoulder obtained using a solution of pH 7

The aging of the cytochrome *c* containing samples was examined in detail, as shown in Fig. 5 where the synchronous scan difference spectra were generated by normalising the Nile red SFS for the different matrices and subtracting from the initial spectrum taken after gelation. A significant decrease of the 600–615 nm band is generally observed. In all matrices, except Gelrite, this decrease is concomitant with an enhancement of the 500 nm band and the appearance of a new band centred at 635 nm. However, this new band is negligible in PEG 20k. PEG has been shown to regulate the dipolarity of the media, as well as increasing the mobility of the guest molecules, without altering the pore size by adhering to the pore walls [11]. The 500 nm band becomes prominent only in presence of TMPS or PEG 20k. The behaviour in presence of Gelrite, is unique in that both 550 and 600–615 nm bands decrease with the concomitant appearance of the 635 band. This may relate to its self-gelling properties, which help to template the formation of the silica network [15]. The matrix where the least change during the aging process is observed, *via* the SFS of the probe, is the GTPES containing one. In this case there is a 20% decrease at 600 nm, with a concomitant increase at 635 nm. Thus this band is indicative of some degree of protein unfolding. However, this occurrence does not compromise the activity of the protein, as shown in next section. Previous work has shown that modification with glycerol based molecules has led to reduced shrinkage and milder reaction conditions [14], while helping to produce preferential interactions between the incorporated protein and host [37, 38]. It was expected that addition of other silanes could reduce the present and influence of unreacted hydroxyl groups [10].

Catalytic activity

To mimic the conditions used for the sol–gel derived media, a solution study was performed with a fixed concentration of H_2O_2 and ABTS, and various concentrations of cytochrome *c*. The result of the kinetic study, examined at 415 nm to monitor the formation of the ABTS radical [10], is given in Fig. 6. From these curves, the initial velocity (v_0) [4] for the catalytic reaction was calculated (by taking the derivative) and is given in Table 1 for use in comparison with the sol–gel derived samples. It was expected that our results would be obtained in a regime where the amount of substrate would be in excess in relation to the amount of cytochrome *c*. Curve A in Fig. 6, shows an initial rapid increase, followed by a

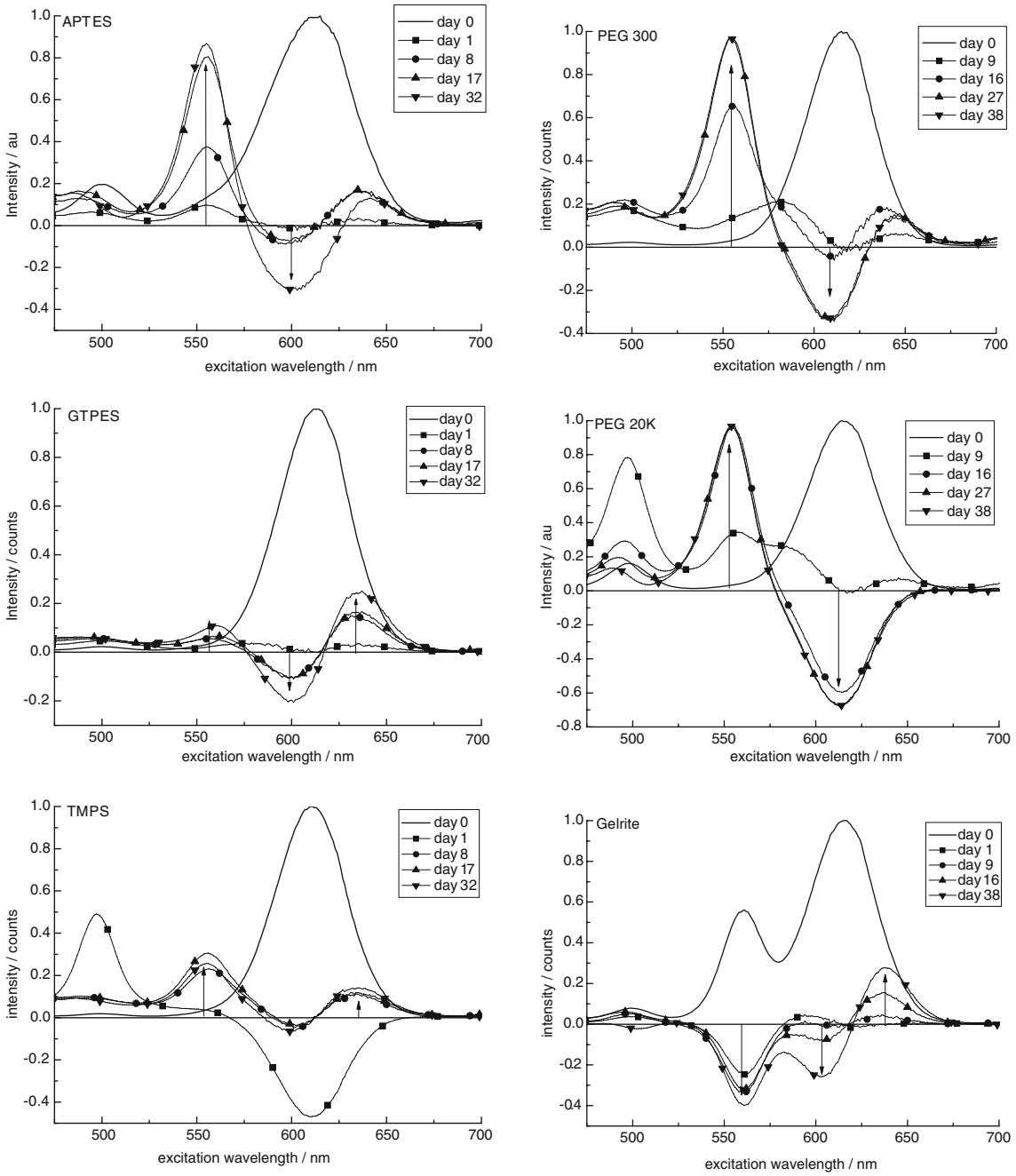

Fig. 5 Comparison of Nile red difference SFS in cytochrome *c* with sol–gel aging time when incorporated into both silane and polymer modified hosts

decrease (also observed in some of the other kinetic curves) which relates to the fact that this reaction is reversible [10].

An example of the kinetic curves for the formation of the ABTS radical at various points during the aging process, in this case APTES, is given in Fig. 7. This shows that the amount of radical formed over the period of the experiment is similar in magnitude to the lower concentrations of cytochrome *c* employed in the solution study. There is a general trend for the amount of radical formed during the time of the experiment to reduce with aging time. However, when comparing the values for the initial velocity from the modified sol–gel hosts over the period of this study (Fig. 8), the sol–gel derived media exhibit v_0 values two orders of magnitude lower than those observed in the solution data (Table 1). It should be kept in mind that slices taken from a monolith are used to perform these measurements rather than powders. This can partially explain the lower values of v_0 obtained compared to free cytochrome *c* [4]. Considering

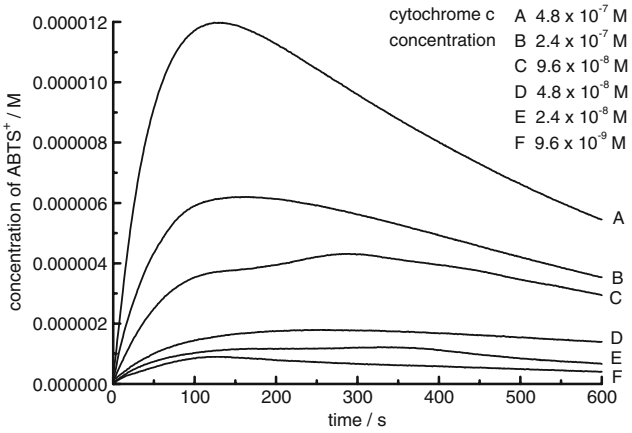

Fig. 6 Catalytic activity in solution, with fixed substrate and H_2O_2 concentrations and varying amounts of cytochrome *c*. The kinetics were monitored at 415 nm

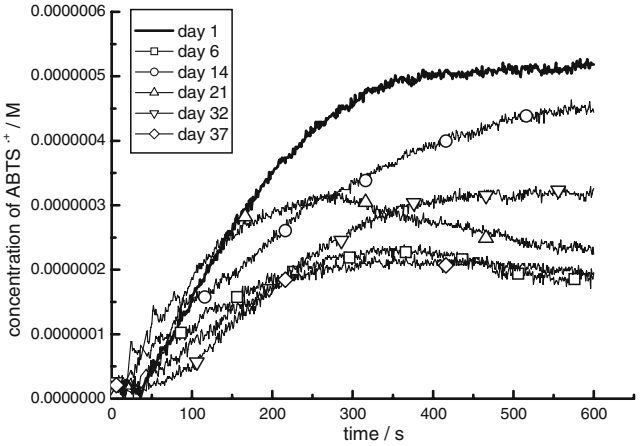

Fig. 7 Catalytic activity with aging time for cytochrome *c* in an APTES modified host

that the spectral data do not show significant unfolding of the protein, then other scenarios to explain the lower v_0 values are required. These include the accessibility within the host, as well as accessibility to the active site once the substrate has encountered the protein within the sol–gel derived media. The fact that a charged radical is formed in the reaction and that this has to exit the matrix before it is spectroscopically detected is also a factor to be considered.

It is evident from Fig. 8, that there is a trend for the initial velocity to decrease with aging time. However, because of the small amount of ABTS radical formed, and associated low absorption values, there is a reasonable error in the dataset. The first set of activity measurements shows that the cytochrome *c* in the different media exhibits similar initial velocities, the main exception is that of the TMPS modified sol–gel host, which consistently displays a lower v_0 and eventually drops to 98% of its initial value. The other silane modified hosts fare better, with a comparative decrease between the first and last measurements of about two thirds of the initial v_0 value. A similar behaviour is seen in the Gelrite modified host. Both of the PEG modified media exhibit the same relative reduction in v_0 (by ~85%). Much of the changes in the values occur within the first couple of weeks of aging, where the vast majority of the morphological changes in these media occur. This is in agreement with what we have seen by fluorescence probing of a similar sol–gel derived medium [39].

Table 1 Initial velocities (v_0) for the ABTS, H_2O_2, cytochrome *c* system for varying concentrations of cytochrome *c*

[Cytochrome *c*] (M)	v_0 (M s^{-1})
9.6×10^{-9}	2.36×10^{-8}
2.4×10^{-8}	3.33×10^{-8}
4.8×10^{-8}	2.63×10^{-8}
9.6×10^{-8}	5.70×10^{-8}
2.4×10^{-7}	1.33×10^{-7}
4.8×10^{-7}	2.53×10^{-7}

Correlation between spectral and catalytic data

In order to help explain the results in the previous sections we have explored the possibility that there exists a connection between the SFS and initial velocity data. The possible factors that we can envisage to explain the catalytic activity data are changes in the protein structure and access of the substrate to the protein. The former relates to the cytochrome itself, while the latter is more influenced by the host. If it is assumed that increases in the SFS 635 nm band and decreases in the 600–615 nm band are assigned to unfolding of the protein, it should be possible to use the relative importance of the 600–615 nm band as a measure of protein conformation changes. Regarding the activity measurements, these are influenced by the conformation of the protein and its accessibility, with the latter

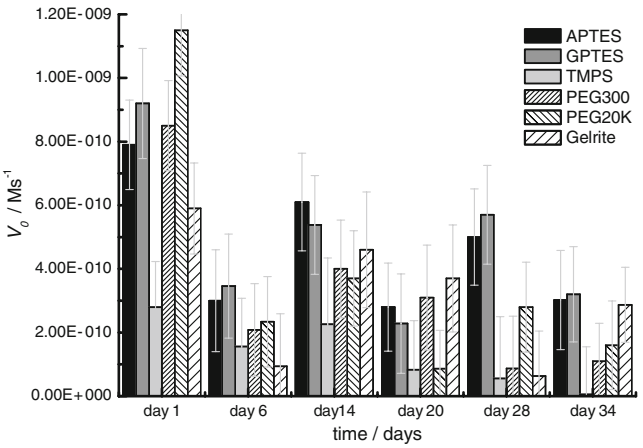

Fig. 8 Comparison of initial velocity (v_0) of the catalytic reaction with aging time for the differently modified matrices

Table 2 Comparison of the reduction in v_0 (in relation to the first activity measurement) with that of the SFS band situated between 600 and 620 nm (in relation to the just gelled spectra) for the last dataset for the differently modified media

Additive	% Reduction in v_0	Average decrease per day ($\times 10^{-12}$ M s^{-1})	% Reduction in SFS band
APTES	62	9.4	37
GPTES	65	9.4	20
TMPS	98	7.5	8
PEG 300	87	16.5 (6.9)[a]	34
PEG 20k	86	20.4 (2.8)[a]	67
Gelrite	51	6.9	26

The decrease in v_0 obtained from a linear fit to all the data is also given to provide an indication of the average decrease per day over the study period

[a] The bracketed number was obtained omitting day 1 data points

affecting the rate of radical formation, reflected in the v_0 value. Considering the first (just after gelation) and final measurements, then any difference between these values should reflect the influence of the host.

Table 2 shows that, overall, the reduction in v_0 is significantly higher than the reduction exhibited by the 600–615 nm band. This difference is most dramatic for the TMPS modified host, which, according to the present hypothesis, means that although this matrix appears suitable for retaining the cytochrome *c* conformation (relatively small changes in SFS—see Fig. 5), it provides poor accessibility for the cytochrome to react with the ABTS and hydrogen peroxide. Both the GTPES and PEG 300 modified hosts show the next biggest difference between our two chosen parameters, with the other modified media exhibiting similar differences. It should be noted that the major changes in the PEG containing host occur within the first week and that the average decreases in v_0 values for all host are more comparable. When combining all the data, these observations allow us to suggest that the Gelrite modified host appears to exhibit the most promising properties probably related to the templating properties of this polysaccharide [15]. This approach shows that it is possible to make a good comparison, making use of Nile SFS and activity measurements, between the modified sol–gel derived media.

Summary

Cytochrome *c* was successfully incorporated into differently modified sol–gel derived hosts without inducing significant structural changes. The conformation was monitored via the use of Nile red synchronous fluorescence spectra. This technique allowed changes in micropolarity to be sensed and indicated some protein unfolding upon incorporation to the host media. The (hydrophobic) probe stays entrapped within different environments in the protein and does not leach to any appreciable extent into the matrix pores, throughout the aging process which lasted several weeks. Measurements of catalytic activity, as reflected by the initial velocity, showed a reduction during the aging process. This effect was ascribed mainly to mass transport increased restrictions, as the building of the silica matrix progresses. When combining the two sets of data, it was possible to discriminate changes attributed to alterations in the protein conformation from the mass transport restrictions ascribed to the aging of the host.

Acknowledgement The Fundação para a Ciência e a Tecnologia is acknowledged for financial support through the PhD grant SFRH/BD/27933/2006.

References

1. Hench LL, West JK (1992) The sol–gel process. Chem Rev 90:33–72
2. Brinker CJ, Scherer GW (1989) Sol–gel science. Academic, New York
3. Dunn B, Miller JM, Dave BC, Valentine JS, Zink JI (1998) Strategies for encapsulating biomolecules in sol–gel matrices. Acta Mater 46:737–741
4. Pierre AC (2004) The sol–gel encapsulation of enzymes. Biocat Biotransform 22:145–170
5. Jin W, Brennan JD (2002) Properties and applications of proteins encapsulated within sol–gel derived materials. Anal Chim Acta 461:1–36
6. Gupta R, Chaudhury NK (2007) Entrapment of biomolecules in sol–gel matrix for applications in biosensors: problems and future prospects. Biosen Bioelect 22:2387–2399
7. Kandimalla VB, Tripathi VS, Ju H (2006) Immobilization of biomolecules in sol–gels: Biological and analytical applications. Crit Rev Anal Chem 36:73–106
8. Livage J, Coradin T, Roux C (2001) Encapsulation of biomolecules in silica gels. J Phys: Condens Matter 13:R673–R691
9. Besanger TR, Brennan JD (2006) Entrapment of membrane proteins in sol–gel derived silica. J Sol–Gel Sci Tech 40:209–225
10. Kadnikova EN, Kostić NM (2002) Oxidation of ABTS by hydrogen peroxide catalysed by horseradish peroxidase encapsulated into sol–gel glass. Effects of glass matrix on reactivity. J Mol Catal B Enzym 18:39–48
11. Baker GA, Jordan JD, Bright FV (1998) Effects of poly(ethylene glycol) doping on the behaviour of pyrene, rhodamine 6G, and acrylodan-labeled bovine serum albumin sequestered within tetramethylorthosilane-derived sol–gel-processed composites. J Sol–Gel Sci Tech 11:43–54
12. Miao Y, Tan SN (2001) Amperometric hydrogen peroxide biosensor with silica sol–gel/chitosan film as immobilization matrix. Anal Chim Acta 437:87–93
13. Gill I, Ballesteros A (1998) Encapsulation of biologicals within silicate, siloxane, and hybrid sol–gel polymers: an effective and generic approach. J Am Chem Soc 120:8587–8598
14. Brook MA, Chen Y, Guo K, Zhang Z, Brennan JD (2004) Sugar modified silanes: precursors for silica monoliths. J Mat Chem 14:1469–1479

15. Shchipunov YA, Karpenko TY (2004) Hybrid polysaccharide-silica nanocomposites prepared by the sol–gel technique. Langmuir 20:3882–3887
16. Bottini M, Di Venere A, Lugli P, Rosato N (2004) Conformation and stability of myoglobin in dilute and crowded organically modified media. J Non-Crystal Solid 343:101–108
17. Kim NH, Jeong MS, Choi SY, Kang JH (2004) Peroxidase activity of cytochrome *c*. Bull Korean Chem Soc 25:1889–1892
18. Yu C-A, Yu L, King TE (1975) Studies on cytochrome *c* oxidase. J Biol Chem 250:1383–1392
19. Dunn B, Zink JI (1997) Probes of pore environment and molecule–matrix interactions in sol–gel materials. Chem Mater 9:2280–2291
20. Savini I, Santucci R, Di Venere A, Rosato N, Strukul G, Pinna F, Avigliano L (1999) Catalytic and spectroscopic properties of cytochrome-*C*, horseradish peroxidase, and ascorbate oxidase embedded in sol–gel silica matrix as a function of gelation time. Appl Biochem Biotech 82:227–241
21. Greenspan P, Fowler SD (1985) Spectrofluorometric studies of the lipid probe, Nile red. J Lipid Res 26:781–789
22. Deye JF, Berger TA, Anderson AG (1990) Nile red as a solvatochromic dye for measuring solvent strength in normal liquids and mixtures of normal liquids with supercritical and near critical fluids. Anal Chem 62:615–622
23. Ghoneim N (2000) Photophysics of Nile red in solution steady state spectroscopy. Spectrochim Acta A 56:1003–1010
24. Hungerford G, Rei A, Ferreira MIC (2006) Use of fluorescence to monitor the incorporation of horseradish peroxidase into a sol–gel derived medium. Biophys Chem 120:81–86
25. Hungerford G, Rei A, Ferreira MIC (2005) Studies on the interaction of Nile red with horseradish peroxidase in solution. FEBS J 272:6161–6169
26. Rubio S, Gomez-Hens A, Valcarcel M (1986) Analytical applications of synchronous fluorescence spectroscopy. Talanta 33:633–640
27. Vo-Dinh T (1978) Multicomponent analysis by synchronous luminescence spectrometry. Anal Chem 50:396–401
28. Ivanov AI, Gavrilov VB, Furmanchuk DA, Aleinikova OV, Konev SV, Kaler GV (2002) Fluorescent probing of the ligand-binding ability of blood plasma in the acute-phase response. Clin Exp Med 2:147–155
29. Hungerford G, Rei A, Ferreira MIC, Suhling K, Tregidgo C (2007) Diffusion in a sol–gel derived medium with a view towards biosensor applications. J Phys Chem B 111:3558–3562
30. Flora KK, Brennan JD (2001) Characterization of the micro-environments of PRODAN entrapped in tetraethyl orthosilicate derived glasses. J Phys Chem B 105:12003–12010
31. Childs RE, Bardsley WG (1975) The steady-state kinetics of peroxidase with 2,2¢-azino-di-(3-ethyl-benzthiazoline-6-sulphonic acid) as chromogen. Biochem J 145:93–103
32. Viseu TMR, Hungerford G, Coelho AF, Ferreira MIC (2003) Dye–host interactions for local effects recognition in homogeneous and nanostructured media. J Phys Chem B 107:13300–13312
33. Cser A, Nagy K, Biczók L (2002) Fluorescence lifetime of Nile red as a probe for the hydrogen bonding strength with its microenvironment. Chem Phys Lett 360:473–478
34. Sackett DL, Wolff J (1987) Nile red as a polarity-sensitive fluorescence probe of hydrophobic protein surfaces. Anal Biochem 167:228–234
35. Baglioni P, Fratini E, Lonetti B, Chen SH (2004) Structural arrest in concentrated cytochrome c solutions: the effect of pH and salts. J Phys Condens Matter 16:S5003–S5022
36. Yonetani T (1967) Studies on cytochrome *c* peroxidase. X. Crystalline apo- and reconstituted holoenzymes. J Biol Chem 242:5008–5013
37. Sui X, Cruz-Aguado JA, Chen Y, Zhang Z, Brook MA, Brennan JD (2005) Properties of human serum albumin entrapped in sol–gel-derived silica bearing covalently tethered sugars. Chem Mater 17:1174–1182
38. Brennan JD, Benjamin D, DiBattista E, Gulcev MD (2003) Using sugar and amino acid additives to stabilize enzymes within sol–gel derived silica. Chem Mater 15:737–745
39. Hungerford G, Rei A, Ferreira MIC, Tregidgo C, Suhling K (2007) Molecular diffusion within sol–gel derived matrices viewed via fluorescence recovery after photobleaching. Photochem Photobiol Sci 6:825–828